

face thermal motion which will tend to mask the rainbow. The high energies used here tend to minimize this averaging effect. Trajectory calculations on model systems are underway to help in the interpretation of this phenomenon.

From a variety of evidence presented above we conclude that for the conditions employed in this study NO undergoes direct inelastic scattering. Qualitatively the results are consistent with a picture based on a strong attractive interaction, a small surface corrugation, and a highly anisotropic repulsive interaction. Further work is required on the role of anisotropy in the attractive potential as well as quantitative comparison of the results with theoretical calculations. By such comparison, measurements of the type presented here can provide detailed information on the potentials and dynamics of molecular interactions with surfaces.

It is our pleasure to acknowledge the expert technical assistance provided by J. E. Schlaegel and V. T. Maxson during the course of these measurements.

<sup>1</sup>D. Auerbach, C. Becker, J. Cowin, and L. Wharton, *Appl. Phys.* **14**, 141 (1977); K. C. Janda, J. E. Hurst, C. A. Becker, J. P. Cowin, L. Wharton, and D. J. Auerbach, *Surf. Sci.* **93**, 270 (1980).

<sup>2</sup>J. A. Barker, private communication; J. C. Tully, *Annu. Rev. Phys. Chem.* **31**, 319 (1980).

<sup>3</sup>F. Frenkel, J. Hager, W. Krieger, H. Walther, C. T. Campbell, G. Ertl, H. Kuipers, and K. Segner, *Phys. Rev. Lett.* **46**, 152 (1981).

<sup>4</sup>G. M. McClelland, G. D. Kubiak, H. G. Rennagel, and R. N. Zare, *Phys. Rev. Lett.* **46**, 831 (1981).

<sup>5</sup>J. C. Polanyi, private communication.

<sup>6</sup>J. E. Hurst, C. A. Becker, J. P. Cowin, K. C. Janda, L. Wharton, and D. J. Auerbach, *Phys. Rev. Lett.* **43**, 1175 (1979); K. C. Janda, J. E. Hurst, C. A. Becker, J. P. Cowin, L. Wharton, and D. J. Auerbach, *J. Chem. Phys.* **72**, 2403 (1980).

<sup>7</sup>Frank O. Goodman and Harold Y. Wachman, *Dynamics of Gas-Surface Scattering* (Academic, New York, 1976).

<sup>8</sup>P. J. Goddard, J. West, and R. M. Lambert, *Surf. Sci.* **71**, 447 (1978).

<sup>9</sup>W. Schepper, U. Ross, and D. Beck, *Z. Phys. A* **290**, 131 (1979).

<sup>10</sup>K. Bergman, U. Hefter, and J. Witt, *J. Chem. Phys.* **72**, 4777 (1980).

<sup>11</sup>R. Schinke, *Chem. Phys.* **34**, 65 (1978).

## Measurement of the Anomalous Nuclear Magnetic Moment of Trivalent Europium

R. M. Shelby and R. M. Macfarlane

*IBM Research Laboratory, San Jose, California 95193*

(Received 17 August 1981)

An order-of-magnitude reduction of the nuclear magnetic moment of trivalent europium due to hyperfine-induced magnetic shielding was predicted by Elliott in 1957. With use of optical hole burning and optically detected nuclear quadrupole resonance in  $\text{YAlO}_3:\text{Eu}^{3+}$ , this shielding has been measured for the first time. We find that the ground-state moment is reduced to 21% of its intrinsic value, while the moment in the excited  ${}^5D_0$  state is unaffected.

PACS numbers: 76.70.Hb, 35.10.Di, 35.10.Fk

More than twenty years ago Elliott<sup>1</sup> predicted that the nuclear magnetic moment of the trivalent europium ion in its ground  ${}^7F_0$  state would be anomalously small. The reason for this is that the electronic contribution to the moment due to second-order hyperfine coupling with the  ${}^7F_1$  levels  $\sim 400\text{ cm}^{-1}$  higher in energy is of opposite sign to, and almost cancels, the intrinsic moment of the Eu nucleus. Since the  ${}^7F_0$ - ${}^7F_1$  splitting is spin-orbit in origin and does not vary greatly from host to host, this cancellation is expected to be a general phenomenon with small modifications depending on the crystalline en-

vironment. As Elliott pointed out, this effect makes conventional NMR or nuclear quadrupole resonance (NQR) observations of trivalent europium very difficult and no such experiments have yet been reported. For this reason Elliott's prediction of the small  $\text{Eu}^{3+}$  moment has, until now, remained unconfirmed.

In  $\text{YAlO}_3:\text{Eu}^{3+}$  we have used hole burning and optically detected NQR in an external magnetic field parallel to the  $b$  axis to measure the effective nuclear moment of  ${}^{151}\text{Eu}$  and  ${}^{153}\text{Eu}$  in both the ground  ${}^7F_0$  and the excited  ${}^5D_0$  states. In the  ${}^7F_0$  state we obtain values of  $0.743\mu_N$  for  ${}^{151}\text{Eu}$  and

TABLE I. Quadrupole splittings of  $\text{Eu}^{3+}$  in  $\text{YAlO}_3$  (MHz).

	${}^7F_0$	${}^5D_0$
${}^{151}\text{Eu}$	45.99 23.03 $\left( \begin{array}{l}  P =11.5 \text{ MHz} \\ \eta=0.03 \end{array} \right)$	89 61 $\left( \begin{array}{l}  P =23.4 \text{ MHz} \\ \eta=0.55 \end{array} \right)$
${}^{153}\text{Eu}$	119.20 59.65 $\left( \begin{array}{l}  P =29.9 \text{ MHz} \\ \eta=0.04 \end{array} \right)$	226 156 $\left( \begin{array}{l}  P =59.6 \text{ MHz} \\ \eta=0.57 \end{array} \right)$

$0.314\mu_N$  for  ${}^{153}\text{Eu}$  corresponding to 21% of the intrinsic moment. These values are used to derive a radial hyperfine parameter  $\langle r^{-3} \rangle = 49.6 \pm 1 \text{ \AA}^{-3}$  which compares well with the best available theoretical value<sup>2</sup> of  $49 \text{ \AA}^{-3}$ . The  ${}^5D_0$  state, on the other hand, shows splittings corresponding to the bare Eu nuclear moment. This is expected since the  $J=1$  level in this case is much further away ( $\sim 2000 \text{ cm}^{-1}$ ). We also find that the quadrupole spin Hamiltonian parameters for the  ${}^5D_0$  and  ${}^7F_0$  states are quite different, reflecting the different contributions of excited  $f$  and  $p$  electron configurations to the quadrupole coupling.<sup>3,4</sup>

Recently we reported<sup>5</sup> the observation of hole burning in  $\text{EuP}_5\text{O}_{14}$ . This involved optical pumping of the ground-state nuclear quadrupole levels, similar to that recently observed in  $\text{Pr}^{3+}$  systems.<sup>6,7</sup> We have chosen  $\text{YAlO}_3:\text{Eu}^{3+}$  for the cur-

rent study because the much better resolution obtained in the hole-burning spectrum allowed the quadrupole splittings to be unequivocally assigned and thus the effective magnetic moment to be more readily determined.

Holes were burned in the inhomogeneously broadened  ${}^7F_0 \leftrightarrow {}^5D_0$  transition of  $\text{YAlO}_3:\text{Eu}^{3+}$  at  $5818 \text{ \AA}$  by irradiating for  $\sim 0.1$  sec with  $\sim 50$  mW of single-frequency laser light in a 1-mm-diam beam. The lifetime of these holes is determined by Eu nuclear spin-lattice relaxation and is  $> 1$  h. The holes were recorded by attenuating the laser ( $\times 10^{-4}$ ) and scanning through the spectrum while monitoring  ${}^5D_0 \rightarrow {}^7F_1$  fluorescence (see Fig. 1). In addition to the hole at the original burning frequency, side holes appear at frequencies corresponding to transitions from the pumped ground-state levels to all excited-state levels. Thus, the positions of the side holes directly give the two  ${}^5D_0$  quadrupole splittings and their sum for each Eu isotope. These results are shown in Table I. As expected, the ratio of the splittings for the two isotopes is equal to the ratio of the quadrupole moments determined by Krebs and Winkler,<sup>8</sup> i.e.,  $Q({}^{153}\text{Eu})/Q({}^{151}\text{Eu}) = 2.54$ . The asymmetry parameter describing the strength of the nonaxial component of the quadrupole tensor is  $\eta = 0.56$ . The enhanced absorptions or antiholes correspond to sums and differences of ground- and excited-state splittings and will be discussed below.

The splitting of the quadrupole levels in an ex-

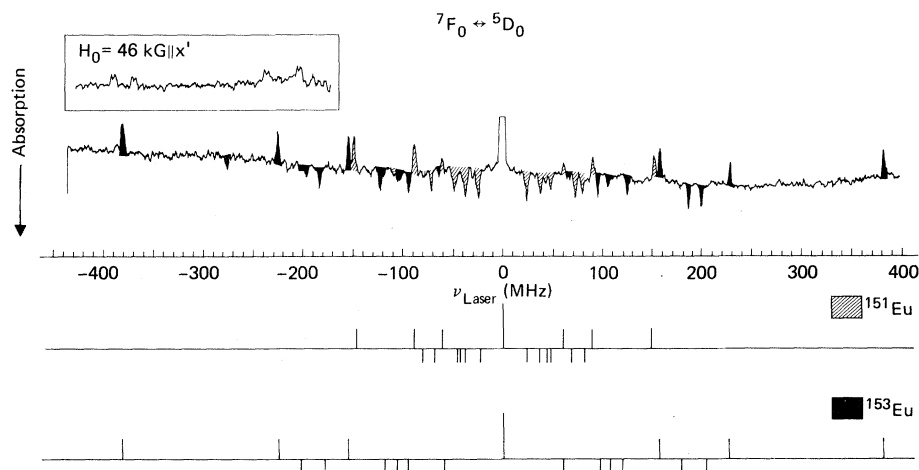


FIG. 1. Hole-burning spectrum of  $\text{YAlO}_3:\text{Eu}^{3+}$  at 1.5 K. The solid-colored peaks are assigned to  ${}^{153}\text{Eu}$  and the cross-hatched peaks to  ${}^{151}\text{Eu}$ . The lower part of the figure shows the positions of the holes and antiholes predicted from the quadrupole splittings shown in Table I. The inset shows hole splittings for  ${}^{153}\text{Eu}$  produced by an external magnetic field.

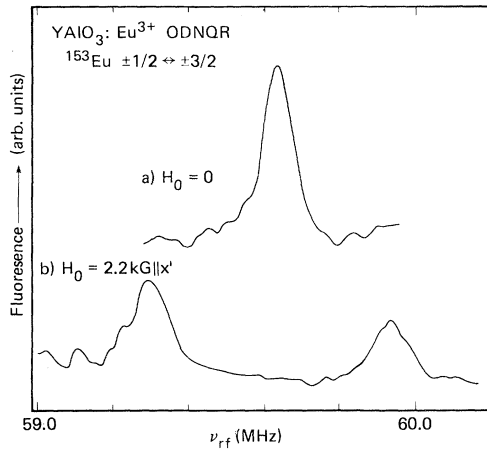


FIG. 2. Curve *a*, ODNQR spectrum in the  ${}^7F_0$  level of  ${}^{153}\text{Eu}$ . Curve *b*, splitting in 2.2-kG external field.

ternal magnetic field perpendicular to the mirror plane of the  $C_s$  point group at the Eu site (i.e., parallel to the  $b$  axis) was measured for  ${}^{153}\text{Eu}$  in the excited  ${}^5D_0$  state by monitoring the splitting of side holes (see inset in Fig. 1). The splitting factors for the  $\pm\frac{1}{2}$ ,  $\pm\frac{3}{2}$ , and  $\pm\frac{5}{2}$  levels were 0.45, 0.74, and 0.08 kHz/G, respectively. From the  ${}^{153}\text{Eu}$  moment of  $1.52\mu_N$ ,<sup>9</sup> one predicts 0.49, 0.84, and 0.06 kHz/G for fields parallel to the  $x'$  principal axis of the quadrupole tensor, while for fields along the  $y'$  or  $z'$  principal axes, the calculated splittings were much different and not in agreement with those observed. This established that the principal axis perpendicular to the mirror plane is the  $x'$  axis, and that the splitting factors in the  ${}^5D_0$  state are well accounted for by the intrinsic nuclear moment. (The primed coordinate system is chosen with one axis perpendicular to the mirror plane such that the largest quadrupole splitting is between the nominally  $m_{z'} = \pm\frac{5}{2}$  and  $\pm\frac{3}{2}$  levels.)

The ground-state splittings were obtained by monitoring the increase in fluorescence accompanying hole refilling when rf is applied at one of the ground-state frequencies.<sup>10</sup> The signal obtained for the 59.65-MHz splitting of  ${}^{153}\text{Eu}$  is shown in Fig. 2, curve *a*. This double-resonance technique is very sensitive, and it was possible to locate all four  ${}^7F_0$  quadrupole resonances

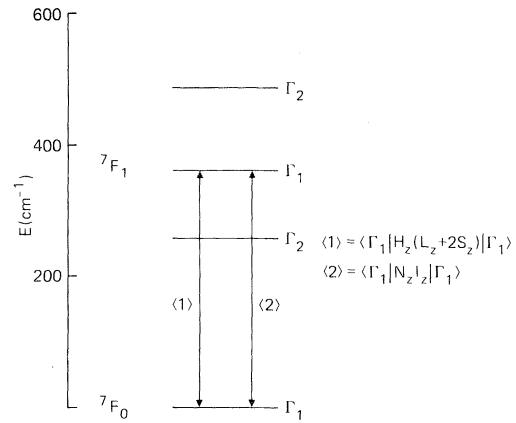


FIG. 3. Level diagram of the  ${}^7F_0(\Gamma_1)$  ground state and the three components of  ${}^7F_1$  showing the interactions responsible for the electronic contribution to the nuclear moment.

which are listed in Table I. The results are again consistent with the known ratio of the nuclear electric quadrupole moments of  ${}^{151}\text{Eu}$  and  ${}^{153}\text{Eu}$ , i.e., 1:2.54.<sup>8</sup> From these frequencies and the  ${}^5D_0$  frequencies, one predicts 21 antihole frequencies for each isotope. However, the overlap factors between the ground-state and excited-state nuclear-spin wave functions indicate that only six of these have significant intensity. The calculated positions of these six are shown for each isotope in the lower part of Fig. 1, and the agreement with the observed spectrum is very good.

Although not required by symmetry, the  ${}^7F_0$  quadrupole tensor is very close to axial ( $\eta = 0$ ). Thus, for fields along  $x'$ , only the  $\pm\frac{1}{2}$  levels will split significantly. This was verified by observing that the  $\pm\frac{3}{2} \leftrightarrow \pm\frac{5}{2}$  transitions did not show measurable splittings for fields  $\leq 50$  kG. In Fig. 2, curve *b*, we show the splitting of the  $\pm\frac{1}{2} \leftrightarrow \pm\frac{3}{2}$  transition for  ${}^{153}\text{Eu}$ . The frequency of the  $+\frac{1}{2} \leftrightarrow -\frac{1}{2}$  transition was also measured as a function of field by the same technique. These measurements gave 0.666 and 0.283 kHz/G for the  $+\frac{1}{2}$  to  $-\frac{1}{2}$  splitting for  ${}^{151}\text{Eu}$  and  ${}^{153}\text{Eu}$ , respectively. This corresponds to effective nuclear moments of  $0.743\mu_N$  and  $0.314\mu_N$ , respectively, which are 0.21 of the intrinsic values ( $3.441\mu_N$  and  $1.52\mu_N$ ).<sup>9</sup>

To analyze this result, we consider the Hamiltonian as given by Elliott<sup>1</sup>:

$$\mathcal{H} = \mu_B \vec{H} \cdot (\vec{L} + 2\vec{S}) + (2\mu_B \mu_N \gamma \hbar) \langle r^{-3} \rangle \vec{N} \cdot \vec{I} - (\hbar \gamma \mu_N) \vec{H} \cdot \vec{I}, \quad (1)$$

where the first term is the electronic Zeeman energy, the second is the magnetic hyperfine interaction, and the third is the nuclear Zeeman energy.  $\vec{H}$  is the external field,  $\vec{L}$  and  $\vec{S}$  the electronic orbital and spin angular momenta,  $\gamma$  the gyromagnetic ratio of the Eu nucleus, and  $2\mu_B \langle r^{-3} \rangle \vec{N}$  is the field

at the nucleus due to the  $f$  electrons, where  $\langle r^{-3} \rangle$  is the average inverse cube of the distance between the electrons and nucleus. As shown in Fig. 3, second-order perturbation theory predicts an admixture into the ground state of the  $\Gamma_1$  component of  ${}^7F_1$ . For magnetic fields perpendicular to the mirror plane, the two  $\Gamma_2$  components are not involved (for discussion of the hyperfine interaction we now use an unprimed coordinate system with the  $z$  axis perpendicular to the mirror plane, i.e.  $\equiv x'$ ). Since this admixture depends on the operator  $I_z$ , a contribution to the nuclear splitting appears, leading to an effective moment given by  $\mu_{\text{eff}} = \hbar I \gamma (1 - \alpha)$ . The reduction factor  $\alpha$  is given by

$$\alpha = [-4\mu_B^2 \langle r^{-3} \rangle \langle \Gamma_1({}^7F_0) | L_z + 2S_z | \Gamma_1({}^7F_1) \rangle \langle \Gamma_1({}^7F_1) | N_z | \Gamma_1({}^7F_0) \rangle] / \Delta \quad (2a)$$

$$= [40\mu_B^2 \langle r^{-3} \rangle] / [3\Delta], \quad (2b)$$

where  $\Delta = 362 \text{ cm}^{-1}$  is the energy of the  $\Gamma_1({}^7F_1)$  level. Therefore, our measurement of  $1 - \alpha = 0.21$  leads to the result  $\langle r^{-3} \rangle = 49.6 \text{ \AA}^{-3}$  with an estimated error of  $\pm 1 \text{ \AA}^{-3}$ . This is in agreement with the best available theoretical value<sup>2</sup> of  $49 \text{ \AA}^{-3}$ .

We note that the two in-plane principal axes of the quadrupole tensor,  $y'$  and  $z'$ , do not necessarily correspond to the  $x$  and  $y$  axes which are defined by the  ${}^7F_1(\Gamma_2)$  wave functions. Thus, there are two contributions to the anisotropy of the low-field splitting factors, corresponding to the orientation of the external field with respect to the quadrupole tensor and to the two  $\Gamma_2$  components which contribute with different energy denominators in Eq. (2b). For fields oriented parallel to the mirror plane, the rotation pattern would have to be carefully analyzed to separate these two effects. Since the  $z$  axis is required by symmetry to be a principal axis of the quadrupole tensor, these complications do not arise for fields in this direction.

The large difference in magnitude and anisotropy of the quadrupole tensor between  ${}^5D_0$  and  ${}^7F_0$  states is attributed to the contribution to the electric field gradient of two important mechanisms, as discussed by Judd, Lovejoy, and Shirley<sup>3</sup> and by Edmonds.<sup>4</sup> Since no quadrupole coupling exists for a pure  $J=0$  level, the observed field gradients are due to admixture of excited states into the  ${}^7F_0$  or  ${}^5D_0$  wave function by the crystal field. The two contributions are of opposite sign<sup>3,4</sup> and are from the excited states of the  $4f^6$  configuration, and from configurations involving excitation of a  $5p$  electron. Elliott<sup>1</sup> estimated the former for europium ethyl sulfate where the crystal field is weaker than in  $\text{YAlO}_3$  and found  $P({}^{153}\text{Eu}) \sim 10$  MHz. This contribution is essentially absent for  ${}^5D_0$  which has no nearby  $J=2$  level. The  $5p$  contribution should be quite similar for both states. Therefore, it is reasonable to attribute the smaller quadrupole coupling for  ${}^7F_0$  to partial cancellation of the  $5p$  contribution by the  ${}^7F_2$  admixture.

The two contributions accidentally result in a net quadrupole coupling which is close to axially symmetric, with the  $z'$  principal axis lying in the mirror plane.

In conclusion, the magnetic shielding of the nuclear magnetic moment of trivalent europium has been measured and is in agreement with a calculation that uses a second-order perturbation formalism as discussed by Elliott.<sup>1</sup> The effective moment is reduced to 21% of its intrinsic value, making its measurement by conventional resonance techniques very difficult. Optically detected nuclear quadrupole resonance provides a sensitive measurement technique and provides information about the excited-state quadrupole coupling as well as that in the ground state. A comparison of the  ${}^7F_0$  and  ${}^5D_0$  quadrupole couplings indicates that the contribution of the  $4f$  electrons is substantial for  ${}^7F_0$ .

The authors wish to thank M. J. Weber for providing the crystal of  $\text{YAlO}_3:\text{Eu}^{3+}$ , and B. Bleaney for making us aware of this problem and for his continued interest in this work. This work was supported in part by the Air Force Office of Scientific Research under Contract No. F49620-79-C-0108.

<sup>1</sup>R. J. Elliott, Proc. Phys. Soc. London, Sect. B **70**, 119 (1957).

<sup>2</sup>B. Bleaney, private communication.

<sup>3</sup>B. R. Judd, C. A. Lovejoy, and D. A. Shirley, Phys. Rev. **128**, 1733 (1962).

<sup>4</sup>D. T. Edmonds, Phys. Rev. Lett. **10**, 129 (1963).

<sup>5</sup>R. M. Macfarlane, R. M. Shelby, A. Z. Genack, and D. A. Weitz, Opt. Lett. **5**, 462 (1980).

<sup>6</sup>L. E. Erickson, Phys. Rev. B **16**, 4731 (1977), and **19**, 4412 (1979).

<sup>7</sup>R. M. Shelby and R. M. Macfarlane, Opt. Commun. **27**, 399 (1978); R. M. Macfarlane and R. M. Shelby, Opt. Lett. **6**, 96 (1981).

<sup>8</sup>K. Krebs and R. Winkler, Naturwissenschaften **21**, 490 (1960).

<sup>9</sup>I. Lindgren, in *Alpha-, Beta-, and Gamma-Ray Spectroscopy*, edited by K. Siegbahn (North-Holland, Amsterdam, 1965), Vol. 2, Appendix 4.

<sup>10</sup>L. E. Erickson, Opt. Commun. **21**, 147 (1977).